Available online at www.sciencedirect.com
SCIENCE DIRECT®
ELSEVIER
Solid State Communications 134 (2005) 97–106
solid state communications
www.elsevier.com/locate/ssc

Quantum coherent effects in cavity exciton polariton systems

Elisabeth Giacobino*, Jean-Philippe Karr, Augustin Baas, Gaétan Messin, Marco Romanelli, Alberto Bramati

Laboratoire Kastler Brossel, Université Pierre et Marie Curie, Ecole Normale Supérieure and CNRS, case 74, 4 place Jussieu, 75252 Paris Cedex 05, France

Received 18 July 2004; accepted 20 July 2004 by guest editors

Available online 6 January 2005

Abstract

The non-linear emission from semiconductor microcavities in the strong coupling regime exhibits specific coherence properties that can be interpreted by parametric polariton four-wave mixing. In a geometry corresponding to degenerate four-wave mixing, we predict and observe a phase dependence of the amplification which is a signature of a coherent polariton wave mixing process. This process is also expected to lead to bistability and squeezed light generation. Spatial effects in the non-linear regime are evidenced, and spatial filtering is required in order to optimize the measured squeezing which is observed close to the bistability turning point. Moreover, the presence of strong coupling inside the microcavity allows to produce a new type of squeezing involving a part-light, part-matter field, the polariton.
© 2004 Published by Elsevier Ltd.

PACS: 71.35.Gg; 71.36.+c; 42.70.Nq; 42.50.−p

Keywords: D. Quantum noise reduction; D. Microcavity polaritons

1. Introduction

In recent years, the optical properties of microcavities containing semiconductor quantum wells in the strong coupling regime [1] have been the subject of detailed investigations. In high finesse semiconductor microcavities with embedded quantum wells [2], the photon and exciton confinement and the large excitonic oscillator strength make it possible to reach the strong coupling regime or normal mode coupling. As a result, the degeneracy at resonance between the exciton mode and the photon mode is lifted and the so-called vacuum Rabi splitting takes place [1]. The resulting two-dimensional eigenstates, called cavity polaritons, are mixed photon–exciton states that have a number of attractive features, especially in the non-linear regime in which strong polariton–polariton scattering takes place. The behaviour of cavity polaritons in the non-linear regime shows the coherent nature of the polariton–polariton interaction, opening the way to quantum effects such as squeezing and quantum correlations. Polaritons are also considered as potential candidates for Bose–Einstein condensation.

The emission intensity of these systems has been shown to undergo a giant amplification when the intensity of the driving field is increased above some threshold, both under non-resonant [3–5] and resonant laser excitation [6–9]. Several mechanisms were proposed to explain this behavior. Experiments using a resonant pump at a specific angle and measuring the amplified emission or the gain on a probe laser at normal incidence [6,8,9], are in good agreement with a recent theoretical model based upon coherent polariton four-wave mixing [10].

A strong amplification is observed when the angle is chosen in order to ensure energy and in-plane momentum

* Corresponding author.
E-mail address: elisabeth.giacobino@cnrs-dir.fr (E. Giacobino).

0038-1098/$ - see front matter © 2004 Published by Elsevier Ltd.
doi:10.1016/j.ssc.2004.07.079

conservation for the process, where two pump polaritons (with momentum $k_{P\|}$ in the plane of the layers) are converted into a signal polariton ($k_{\|}=0$) and an idler polariton ($k_{\|}=2k_{P\|}$). Most studies involving resonant excitation of microcavity polaritons have been performed in a non-degenerate configuration, in which the signal, idler and pump beams have different energies and momenta. Here we will focus on an alternative configuration that ensures the double energy and momentum resonance, the one, where $k_{P\|}=0$, with $k_{\mathrm{signal}\|}=k_{\mathrm{idler}\|}=0$, the energy of the pump laser being resonant with the polariton energy. The amplified emission, which now contains both signal and idler, is observed in the direction of the reflected pump beam. The 'degenerate' configuration allows us to highlight new features of the polariton parametric interaction. To analyze the characteristics of the emission in detail, a highly sensitive homodyne detection is used. As in the non-degenerate case, a marked threshold is observed in the emission when the pump intensity is increased and the associated shift is found to be in agreement with Ref. [10]. Degenerate four-wave mixing has been studied by several authors [11,12] in semiconductor microcavities, however, in different regimes, where the giant amplification on the lower polariton branch did not occur.

It is well known that in this geometry optical parametric amplification is phase sensitive [13]. Using a single mode cw laser as a pump, we have been able to investigate the phase dependence of the giant emission. If it was due to stimulation by the lower polariton occupation number [9], a phase insensitive amplification would be observed, as in a laser-like amplifier [14]. We have observed that the amplification depends strongly on the phase relative to the pump laser. With respect to the phase of the laser beam, some quadrature components of the emitted light are amplified, while other quadrature components are deamplified, bringing in a crucial argument in favor of the interpretation of the amplified emission as originating primarily from coherent polariton four-wave mixing in the case of resonant pumping [18]. Let us note that the case of non resonant pumping [5], where there is no phase reference in the system corresponds to a very different problem which requires a specific approach.

Owing to the coherent nature of the non-linear effect, quantum properties can be expected [15]. Quantum effects such as squeezing of the outgoing light have been predicted and observed in cavities containing atoms [16]. However, the non-classical features must not be destroyed by spurious fluctuations linked to the relaxation processes that are often more effective in semiconductors than in atomic ensembles. Experiments performed in bulk semiconductors with high laser power have demonstrated the possibility to modify the quantum fluctuations and to generate squeezing in semiconductors [17]. Here, we have used the high efficiency of the polariton scattering to demonstrate quantum effects with very low pump laser power. Indeed, the deamplification mentioned above for some specific quadrature components brings the emitted light below the standard quantum noise, thus producing squeezing. Squeezing in the emitted light reveals squeezing of the polariton field inside the cavity [19].

2. Microcavity polaritons

We consider a microcavity containing a semiconductor quantum well embedded between two highly reflecting planar Bragg mirrors separated by a distance of the order of the wave-length. The discussion is limited to a two-band semiconductor. The electromagnetic field can excite an electron from the filled valence band to the conduction band, thereby creating a hole in the valence band. The electron–hole system possesses bound states, the excitonic states [20]. We will only consider the lowest of these bound states, the 1s state. The excitons are confined along the growth direction (z direction) and free in the plane of the layers (xy plane). The excitons couple with the light field in the cavity [2,21]. In a perfect planar cavity, the translation invariance implies a wave vector conservation for the exciton photon coupling. If $K_{\|}$ and $k_{\|}$ are the in-plane wave vectors for the exciton and the photon, respectively, this means $K_{\|}=k_{\|}$. In the following, in order to simplify the notations, we will drop the indices for $K_{\|}$ and $k_{\|}$ and use K and k for the in-plane wave vectors.

2.1. The strong coupling regime

Neglecting the spin degrees of freedom, we can write an effective interaction Hamiltonian for the coupled exciton–photon system in the linear regime:

$$H=\sum_k E_{\mathrm{cav}}(k)a_k^\dagger a_k+\sum_K E_{\mathrm{exc}}(K)b_K^\dagger b_K + \sum_k \frac{\hbar}{2}\Omega_R(a_k^\dagger b_k+b_k^\dagger a_k) \quad (1)$$

The sums over $k=K$ run for the momenta in the cavity plane only. The first two terms correspond to the energies of the photons and of the excitons, where a_k and b_K are, respectively, the annihilation operators of a photon of in-plane momentum k and of an exciton of in-plane momentum K and $E_{\mathrm{cav}}(k)$ and $E_{\mathrm{exc}}(K)$ are the energies of the corresponding cavity and exciton modes. The third term corresponds to the exciton–photon coupling with a strength Ω_R.

The linear Hamiltonian given in (1) can be easily diagonalized for each k value using the polariton basis

$$H_k=E_k^+ p_k^{(+)\dagger}p_k^{(+)}+E_k^- p_k^{(-)\dagger}p_k^{(-)} \quad (2)$$

where the energies of the upper $p_k^{(+)}$ and lower $p_k^{(-)}$ polaritons write

$$E_k^{\pm} = \frac{1}{2}\left(E_{\text{exc}}(k) + E_{\text{cav}}(k) \pm \hbar\sqrt{\delta_k^2 + \Omega_R^2}\right) \tag{3}$$

with

$$\hbar\delta_k = E_{\text{cav}}(k) - E_{\text{exc}}(k) \tag{4}$$

The energies of the upper and lower polaritons are represented in Fig. 1 for $k=0$.

For zero detuning the degeneracy between exciton and cavity is lifted and an anticrossing appears. It is often called the vacuum Rabi splitting [22,23].

The polariton operators are given as functions of the photon and exciton operators as

$$p_k^{(-)} = -C_k a_k + X_k b_k$$

$$p_k^{(+)} = X_k a_k + C_k b_k \tag{5}$$

with

$$X_k^2 = \frac{\delta_k^2 + \sqrt{\delta_k^2 + \Omega_R^2}}{2\sqrt{\delta_k^2 + \Omega_R^2}} \tag{6}$$

$$C_k^2 = \frac{\Omega_R^2}{2\sqrt{\delta_k^2 + \Omega_R^2}\left(\delta_k^2 + \sqrt{\delta_k^2 + \Omega_R^2}\right)} \tag{7}$$

The Hopfield coefficients X_k and C_k represent, respectively, the exciton and photon fractions of the lower polariton, and the photon and exciton fractions of the upper polariton.

The exciton dispersion is given by

$$E_{\text{exc}}(K) = E_{\text{exc}}(0) + \frac{\hbar^2 K^2}{2M} \tag{8}$$

where $E_{\text{exc}}(K)$ the exciton energy with in-plane momentum K and M is the reduced exciton mass for the in-plane motion, and the dispersion of the cavity mode is given by

$$E_{\text{cav}}(k) = \sqrt{E_{\text{cav}}^2(0) + \frac{\hbar^2 c^2 k^2}{n_c^2}} \tag{9}$$

where $E_{\text{cav}}(k)$ the cavity energy for the resonant mode with in-plane momentum k and n_c the index of refraction of the semiconductor. Using the photon and exciton dispersion relations, one can deduce the polariton dispersion, as represented in Fig. 2 for $E_{\text{cav}}(0)=E_{\text{exc}}(0)$.

Now if relaxation phenomena are taken into account, the cavity field and the exciton have finite lifetimes. This can be accounted for in an effective Hamiltonian by introducing complex energies, $E_{\text{cav}}(k)-\text{i}\hbar\gamma_{\text{cav}}(k)$ and $E_{\text{exc}}(k)-\text{i}\hbar\gamma_{\text{exc}}(k)$. The polariton energies are now complex numbers. For zero cavity exciton detuning ($\delta_k=0$), one obtains

$$E_k^{\pm} = E_{\text{exc}}(k) - \frac{\text{i}}{2}\hbar(\gamma_{\text{cav}}(k) + \gamma_{\text{exc}}(k)) \pm \frac{\hbar}{2} \times \sqrt{\Omega_R^2 - (\gamma_{\text{cav}}(k) - \gamma_{\text{exc}}(k))^2} \tag{10}$$

It can be seen that if Ω_R is larger than the difference of the relaxation rates, the degeneracy is actually lifted between the two eigenstates: it is the strong coupling regime. If the coupling coefficient Ω_R^2 is not large enough, the vacuum Rabi splitting disappears and the system is in the weak coupling regime.

2.2. Non-linear effects and quantum treatment of the cavity polaritons

When the number of photons and excitons is not very small, additional interaction terms must be considered in the Hamiltonian (1). The main effect is the collision between two excitons, giving rise to two other excitons. The corresponding term in the Hamiltonian writes [24,25]

$$H_{\text{NL}} = \frac{1}{2}\sum_{K,K'}\sum_{Q} V_0 b_K b_{K'} b_{K+Q} b_{K'-Q} \tag{11}$$

It describes the exciton–exciton scattering due to Coulomb interaction, with $V_0 = 6e^2 a/\varepsilon_0 A$, where a is the two-dimensional Bohr radius of the exciton and A the quantization area. This term is at the origin of the non-linear behavior in the microcavity.

In the following, the treatment will focus on the case of only one photon mode irradiating the microcavity, with

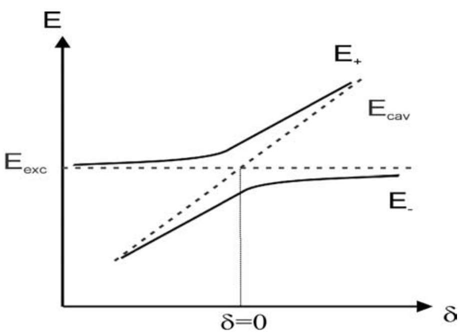

Fig. 1. Energies of the two polariton branches for $k=0$, as a function of the detuning δ between the cavity and the exciton.

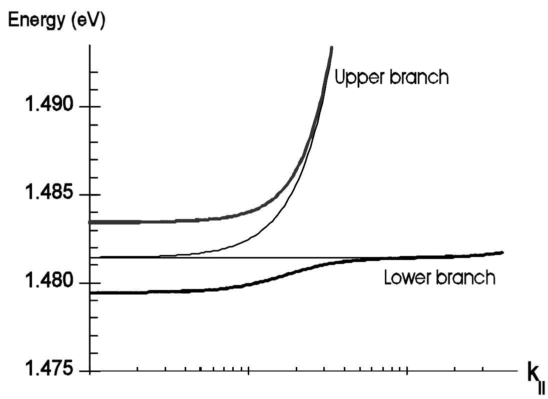

Fig. 2. Dispersion of the two polariton branches, as a function of the in-plane wave number $k_{\|}$.

$k=0$. Because of the in-plane momentum conservation in the exciton–photon interaction, this cavity mode is only coupled with one exciton mode of $K=0$. Using Eqs. (1) and (11) with $K=K'=Q=0$ the Hamiltonian of the coupled system can be written as:

$$H = E_{\mathrm{cav}} a^{\dagger} a + E_{\mathrm{exc}} b^{\dagger} b + \frac{\hbar}{2} \Omega_R (a^{\dagger} b + b^{\dagger} a) + \frac{1}{2} V_0 b^{\dagger} b^{\dagger} b b \tag{12}$$

with $E_{\mathrm{cav}}=E_{\mathrm{cav}}(0)$ and $E_{\mathrm{exc}}=E_{\mathrm{exc}}(0)$ and where the indices $k=0$ have been left out. This Hamiltonian can also be written in the polariton basis. We will assume that the non-linear term is small and neglect the non-diagonal terms of the non-linear Hamiltonian between the upper and lower polariton. Then we can write a Hamiltonian for the lower polariton only

$$H = E_{\mathrm{LP}} p_0^{\dagger} p_0 + \frac{1}{2} (V^{\mathrm{eff}} p_0^{\dagger} p_0^{\dagger} p_0 p_0) \tag{13}$$

where p_0 is the annihilation operator for the lower polariton at $k=0$, E_{LP} is the lower polariton energy and $V^{\mathrm{eff}}=X_0^4 V_0$.

From the form of the non-linear part of the Hamiltonian (13), the quantum optical properties of the polariton are expected to be analogous to that of a Kerr medium in an optical cavity, which is the same as degenerate four-wave mixing in a cavity.

Using the input output formalism [26] we can write a Heisenberg–Langevin equation for the lower polariton (in the frame rotating at the driving laser frequency ω_{L})

$$\frac{\mathrm{d}}{\mathrm{d}t} p_0 = -(\gamma_0 + \mathrm{i}\delta_0) p_0 - \mathrm{i}\alpha p_0^{\dagger} p_0 p_0 + \sqrt{2\gamma_0} P^{\mathrm{in}} \tag{14}$$

where γ_0 is the polariton linewidth, $\delta_0 = E_{\mathrm{LP}}/\hbar - \omega_{\mathrm{L}}$, $\alpha = V^{\mathrm{eff}}/\hbar$, P^{in} is the polariton input term. The polariton input term can be deduced from the equations for the cavity photons and excitons

$$\sqrt{2\gamma_0} P^{\mathrm{in}} = -C_0 \sqrt{2\gamma_{\mathrm{cav}}} A^{\mathrm{in}} + X_0 \sqrt{2\gamma_{\mathrm{exc}}} B^{\mathrm{in}} \tag{15}$$

where γ_{cav} and γ_{exc} are the cavity and exciton linewidths, A^{in} and B^{in} are the photonic and excitonic input terms and X_0 and C_0 the Hopfield coefficients. The lower polariton relaxation rate is given by

$$\gamma_0 = C_0^2 \gamma_{\mathrm{cav}} + X_0^2 \gamma_{\mathrm{exc}} \tag{16}$$

We are now going to use this evolution equation to study on the one hand the reflected and transmitted laser fields, and on the other hand the emission, which is made of fluctuating fields with zero mean value.

3. Steady-state regime: bistability and spatial effects

Using Eq. (14), the mean values of the polariton field inside the microcavity and of the optical field outside can easily be calculated. We rewrite the equation for the mean fields, using the fact that the only input term with a non-zero mean value is the driving laser field A^{in} and we solve it for the stationary regime:

$$\frac{\mathrm{d}\langle p_0\rangle}{\mathrm{d}t} = -(\gamma_0 + \mathrm{i}\delta_0)\langle p_0\rangle - \mathrm{i}\alpha n_0 \langle p_0\rangle - C_0 \sqrt{2\gamma_{\mathrm{cav}}} \times \langle A^{\mathrm{in}}\rangle = 0 \tag{17}$$

where $n_0 = |\langle p_0\rangle|^2$ is the mean number of polaritons. Multiplying Eq. (17) by its conjugate, we obtain an equation for n_0

$$n_0(\gamma_0^2 + (\delta_0 + \alpha n_0)^2) = 2\gamma_{\mathrm{cav}} C_0^2 I^{\mathrm{in}} \tag{18}$$

For a range of values of the driving laser power the polariton number is found to have three possible values, the higher and the lower ones been stable, the intermediate one being unstable. A bistable behavior is obtained for positive values of the discriminant, i.e. $\delta_0^2 > 3\gamma_0^2$. Moreover the solutions for n_0 should be positive real numbers. Combining these two conditions, bistability is predicted when

$$\delta_0 < -\sqrt{3}\gamma_0 \tag{19}$$

Bistability can be evidenced by scanning the input intensity for a fixed detuning between the exciton and the cavity and measuring the reflectivity R. Alternatively, it is possible to scan the cavity length for a fixed value of the input intensity, as for atoms in cavity [27]. In a semiconductor microcavity, this can be done by scanning the excitation spot on the sample surface when the cavity is wedged (i.e. there is a slight angle between the Bragg mirrors).

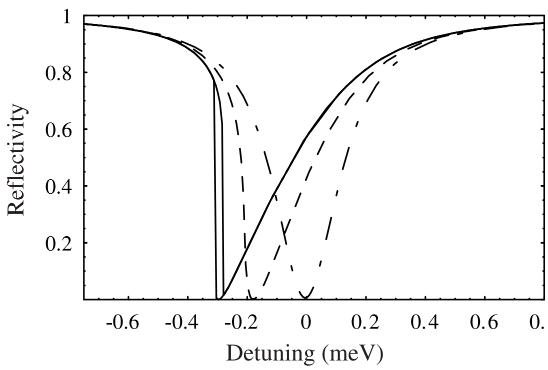

Fig. 3. Calculated reflectivity spectra as a function of the cavity–exciton detuning, for I^{in} near zero (dash–dotted line), $I_{\mathrm{in}}=0.5$ mW (dashed line) and $I^{\mathrm{in}}=1$ mW (solid line). The laser energy is $E_{\mathrm{L}}=E_{\mathrm{exc}}-\hbar_R/2$, equal to the lower polariton energy at zero cavity–exciton detuning in the absence of non-linear effects. The reflectivity resonance is indeed at $\delta=0$ in the low intensity case but it is shifted at higher intensity. For the highest intensity, a hysteresis cycle appears when scanning the spot position in the two directions.

Fig. 3 shows the calculated variations of R with the cavity–exciton detuning for three values of I^{in} (close to zero, below and above the bistability threshold). For the highest intensity, the reflectivity spectrum shows the characteristic hysteresis cycle. The output power switches abruptly when the position of the excitation spot is scanned and it depends on the direction of the scan. The hysteresis cycle can also be seen on the transmission and absorption spectra.

Thus exciton–exciton interaction in semiconductor microcavities is predicted to lead to an optically bistable regime in the vicinity of the polariton resonance. An alternative mechanism for achieving optical bistability was proposed in Refs. [28,29], using the bleaching of the Rabi splitting; in contrast with this case, we obtain the present effect when the exciton–exciton interaction term is much smaller than the Rabi splitting term. We also stress that this mechanism is different from the optical bistability which has been demonstrated in semiconductor microcavities at room temperature [30], since it involves an exciton–photon mixed mode instead of a cavity mode.

The non-linear effects are also associated with spatial effects. Since the thickness of the cavity varies over the surface of the laser spot, the polariton detuning is position dependent within the spot. The spatial effects have been studied experimentally by recording the reflected light with a CCD camera. At low intensity, the resonance region is found to be a straight line. The results at higher intensity can be seen in Fig. 4 for different positions of the excitation spot. The main resonant region can be seen near the center of the spot; depending on the position of the spot, its shape is that of a crescent, a ring or a dot. The shape of the resonance region can be understood as resulting from exact compensation between the non-linear energy shift due to the intensity variations, and the linear energy shift due to the cavity thickness variations. The results of a calculation including the spatial effects are in good agreement with the experimental results of Fig. 4.

In view of these transverse effects, the reflectivity spectrum is better studied by selecting a small zone on the sample in order to avoid averaging the optical response on the spot surface. One solution is to have an excitation spot with a uniform distribution in intensity, sufficiently small for the effect of the cavity wedge to be negligible. Spatial selection can be also easily achieved by spatial filtering of the reflected beam. We have used a spatial filter for the reflected light in order to select only a small fraction of the excitation spot. The filter has the size of the dark absorption dot of Fig. 4, i.e. about 10 μm in diameter. It is with such spatial filtering that bistability was studied. The reflectivity spectra are obtained at fixed excitation energy and intensity, by scanning the spot position over the sample surface. Fig. 5 shows a series of spectra for several values of the excitation intensity.

A shift of the resonance position proportional to the excitation intensity was observed. The resonance position shifts towards negative detunings, corresponding to a blueshift of the resonance energy. This is in agreement

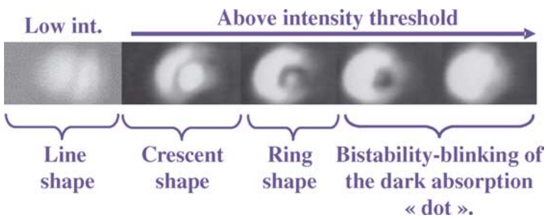

Fig. 4. Near-field images of the reflected beam. The laser wavelength is 831.69 nm, resonant with the lower polariton at $\delta = 0.3$ meV. The first image is taken at very low excitation intensity (0.2 mW). All the other images are taken at 2 mW, for different positions of the excitation spot on the sample. The last two images are obtained for the same position; we observed a blinking between these two states, due to mechanical vibrations.

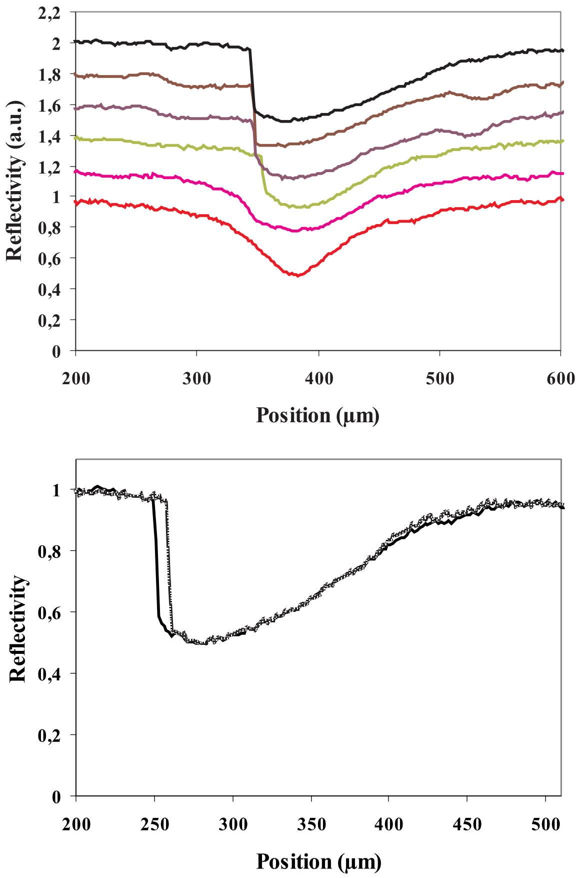

Fig. 5. Upper figure: reflected intensities (in arbitrary units) as a function of the spot position on the sample (the origin of the axis is arbitrary), for several values of the input power I^{in}: 1–6 mW. The laser wavelength is 831.32 nm, resonant with the lower polariton at $\delta = 1.5$ meV. Bistability appears at $I^{in} = 2.8$ mW. Lower figure: hysteresis cycle for the curve $I^{in} = 6$ mW. The two curves correspond to the two directions for the scan of the spot position on the sample.

with the model, where the blueshift is given by Eq. (17). The shift has been removed in Fig. 5, so that all the curves appear to be peaked around the same position.

Above some threshold intensity, one can observe as expected a hysteresis cycle by scanning the sample position in two opposite directions (Fig. 5). The bistability threshold can be determined with a good precision by observing the spontaneous 'blinking' between the two stable values, due to the intensity fluctuations or mechanical vibrations of optical elements on the set-up [31].

4. Study of the emitted light

We now turn to the study of the light emitted by the cavity under laser excitation, i.e. photoluminescence. It consists in a fluctuating field with a non-zero mean intensity but no mean field value. This fluctuating field is also referred to as noise in the following. In order to derive it, we use Eq. (14) with an input term that includes the fluctuating parts of the input fields. Let us stress that the presence of relaxation processes for the polariton implies the existence of incoming fluctuations, due to fluctuation–dissipation theorem. These input fluctuations are at least the vacuum noise.

The input term for the light field A^{in} is the driving laser field introduced above, together with its quantum fluctuations δA^{in} which are equal to the vacuum noise (if the laser is assumed to have no excess noise), so that their correlation function is

$$\langle \delta A^{\mathrm{in}\dagger}(t)\delta A^{\mathrm{in}}(t+\tau)\rangle = \delta(\tau) \tag{20}$$

The input term for the exciton field B^{in} comprises only noise since there is no direct excitation of the exciton field. This input noise is at least equal to the vacuum noise. In addition there is thermal noise coming from phonon interaction. Assuming that the thermal noise is due to an exciton reservoir which is populated by collisions of the pump polaritons with acoustic phonons, the correlation function of the input noise is the sum of two terms: the vacuum noise as for the optical field in Eq. (20), and a term proportional to the number of pump polaritons, that are then transferred by the phonons into the polariton mode of interest at a constant rate [19,32].

$$\langle B^{\mathrm{in}\dagger}(t)B^{\mathrm{in}}(t+\tau)\rangle = (1+\beta n_{\mathrm{b}})\delta(\tau) \tag{21}$$

where n_{b} is the population of the $k=0$ mode due to direct laser excitation and β is the excitation rate of the reservoir. In order to derive the equation for the fluctuations, one linearizes the evolution equation. Starting from Eq. (14), one obtains

$$\frac{\mathrm{d}\delta p_0}{\mathrm{d}t} = -(\gamma_0 + \mathrm{i}\delta_0)\delta p_0 - 2\mathrm{i}\alpha\langle p_0^\dagger p_0\rangle\delta p_0 - \mathrm{i}\alpha\langle p_0 p_0\rangle\delta p_0^\dagger + \sqrt{2\gamma_0}P^{\mathrm{in}} \tag{22}$$

We see that the non-linear interaction term in Eq. (14) yields two terms in the linearized Eq. (22). The first one is proportional to the polariton field intensity and gives a non-linear shift. The second one, involving $\delta p_0^\dagger$ is responsible for the parametric gain, as will be explained below.

The value of β can be evaluated experimentally by measuring the luminescence at very low excitation density. In such conditions the non-linear term in Eq. (22) can be neglected and the emitted field comes from thermal processes and increases linearly with the excitation intensity. This property was verified and the value of β deduced from the slope of the luminescence as a function of the excitation intensity. This is consistent with the linear dependence of photoluminescence with exciting laser intensity observed in other experiments at low driving intensities.

Using Eqs. (20) and (21) for the polariton noise input, we have calculated from Eq. (22) the noise properties of the light going out of the microcavity. This noise is made of a superposition of quadrature components with phases distributed over 2π. In the linear regime this emission has no phase dependence, i.e. all the quadrature components have the same intensities.

As shown in Ref. [18], in the presence of non-linear polariton interaction the noise exhibits a phase dependence, i.e. some quadrature components are amplified while some other quadrature components are deamplified. Using Eq. (22) and of its hermitian conjugate allows to predict the behavior of all the noise quadratures. In order to understand how the phase dependent non-linear amplification appears, we will treat the simpler case of optical parametric amplification that has an analogous behavior.

4.1. Amplification and squeezing in degenerate parametric amplification

The Hamiltonian for parametric amplification in a crystal is, given by Ref. [13]

$$H = \mathrm{i}\hbar\chi^{(2)}a_p a^\dagger a^\dagger + h.c. \tag{23}$$

where $\chi^{(2)}$ is the second-order non-linearity of the crystal, a_p is the pump field and a is the signal field. The process described here is parametric amplification, where one pump photon is annihilated and two identical signal photons are created (degenerate parametric interaction). The parametric crystal is placed in a resonant optical cavity, so that the evolution equation for the field mode inside the cavity is given by a Heisenberg–Langevin Eq. [26] as above with a Hamiltonian term obtained from Eq. (23)

$$\frac{\mathrm{d}a}{\mathrm{d}t} = ga^\dagger - \gamma_{\mathrm{cav}}a + \sqrt{2\gamma_{\mathrm{cav}}}A^{\mathrm{in}} \tag{24}$$

where $g=2\chi^{(2)}\langle a_p\rangle$ is the parametric gain, γ_{cav} is the decay rate of the cavity and the input field A^{in} is the vacuum field. The cavity is resonant with the a field frequency and the equation is written in the frame rotating at the a field frequency.

Since the equation is linear in the quantum field, the equation for the fluctuations is immediately obtained as

$$\frac{\mathrm{d}\delta a(t)}{\mathrm{d}t} = g\delta a^{\dagger}(t) - \gamma_{\mathrm{cav}}\delta a(t) + \sqrt{2\gamma_{\mathrm{cav}}}\delta A^{\mathrm{in}}(t) \quad (25)$$

We shall write the solution in terms of the quadrature components defined by

$$p = (a + a^{\dagger}) \quad (26)$$

$$q = -\mathrm{i}(a - a^{\dagger})$$

We take the Fourier transform of the equations for p and q, which transforms the differential equations into algebraic equations, and allows to easily solve them

$$\delta p(\omega) = \frac{\sqrt{2\gamma_{\mathrm{cav}}}}{\gamma_{\mathrm{cav}} - g - \mathrm{i}\omega}\delta P^{\mathrm{in}}(\omega) \quad (27)$$

$$\delta q(\omega) = \frac{\sqrt{2\gamma_{\mathrm{cav}}}}{\gamma_{\mathrm{cav}} + g - \mathrm{i}\omega}\delta Q^{\mathrm{in}}(\omega)$$

where ω is the noise frequency and $\delta P^{\mathrm{in}}(\omega)$ and $\delta Q^{\mathrm{in}}(\omega)$ are the input quadrature components, defined as in Eq. (26). The field outside the cavity is

$$A^{\mathrm{out}}(\omega) = \sqrt{2\gamma_{\mathrm{cav}}}a(\omega) - A^{\mathrm{in}}(\omega) \quad (28)$$

$$\delta P^{\mathrm{out}}(\omega) = \frac{\gamma_{\mathrm{cav}} + g + \mathrm{i}\omega}{\gamma_{\mathrm{cav}} - g - \mathrm{i}\omega}\delta P^{\mathrm{in}}(\omega) \quad (29)$$

$$\delta Q^{\mathrm{out}}(\omega) = \frac{\gamma_{\mathrm{cav}} - g + \mathrm{i}\omega}{\gamma_{\mathrm{cav}} + g - \mathrm{i}\omega\tau}\delta Q^{\mathrm{in}}(\omega)$$

It is immediately seen that the quadrature component $\delta P^{\mathrm{out}}(\omega)$ is amplified and diverges at zero frequency for $\gamma_{\mathrm{cav}}=g$, while the other quadrature component $\delta Q^{\mathrm{out}}(\omega)$ is deamplified and squeezed below the quantum noise limit if the incoming field is the vacuum. The term responsible for these effects in Eq. (25) is the one that couples δa and $\delta a^{\dagger}$ and thus introduces amplification and deamplification depending on the considered quadrature.

4.2. Non-linear emission and amplification in semiconductor microcavities

It can be seen that the structure of Eq. (22) is quite similar to the one of Eq. (25) except for the second term on the right hand side of Eq. (22), that produces a non-linear shift. Also, the gain is proportional to $\langle p_0^{\dagger}p_0\rangle$ for the polariton case. Actually, the parametric amplifier corresponds to three wave mixing, whereas the microcavity polaritons undergo four-wave mixing. However, the main results are similar.

In the present case of degenerate operation with the emitted signal and idler polaritons having the same energies and wave vectors, phase-dependent parametric amplification is expected. In Eq. (22) thermally excited polaritons represented by the noise input term constitute the probe that seeds the parametric process and which is amplified through

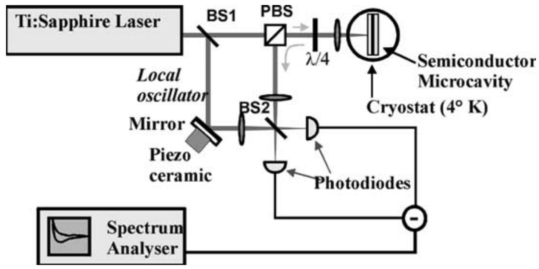

Fig. 6. Experimental set-up. The microcavity sample is excited using a Ti: sapphire laser. The quarter wave plate in front of the sample ensures excitation with a circular polarization. The reflected beam is observed sent towards a homodyne detection set-up. Beamsplitter BS1 allows to take a part of the excitation beam, used as a local oscillator, i.e. recombined on beamsplitter BS2 with the incoming reflected beam.

interaction with the pumped polaritons. Having no average phase, the thermal polaritons can be considered as an ensemble of random polariton fields with equal mean amplitudes and phases spread over 2π. In order to check the predicted properties, the experiment has to allow phase dependent measurements, in contrast to other experiments showing amplification [8].

The emission spectra were studied using a specific method, the so-called homodyne detection method, which is of current use in quantum optics. The light emitted by the microcavity is detected in the direction normal to the sample by means of a homodyne detection system [34,35]. For this purpose the emitted light is mixed with a local oscillator on photodetectors (Fig. 6). More precisely, the emitted light of interest copropagates with the reflected pump laser beam and has the same very small divergence angle ($\simeq 0.4°$). An additional laser beam split off from the same laser as the pump beam by means of a beamsplitter (BS1), the local oscillator, is mixed with the pump and signal beam on a second beamsplitter (BS2). The beams coming from beamsplitter BS2 are focused on two photodetectors. The frequency spectrum of the photocurrent difference is analyzed with an RF spectrum analyzer.

The reflected laser and the light scattered at the laser frequency interfere with the local oscillator and yield a large interference peak at zero frequency which is filtered out. The signal given by the spectrum analyzer can then be shown [35] to be proportional to the beat signal between the local oscillator and the light emitted by the sample, i.e. luminescence. The spectrum analyzer yields the Fourier transform of the emitted light, i.e. the interference spectrum between the local oscillator and the emitted light. Since the emission is incoherent light, the spectrum analyzer measures a very broad signal as a function of frequency, that appears on top of the background quantum noise (shot noise).

The possible frequency scan of the spectrum analyzer is of the order of a few hundred MHz, i.e. in the 100 neV range. This is much narrower than a typical photoluminescence spectrum, and the latter cannot be studied by frequency scanning the spectrum analyzer. Thus, we chose to operate the spectrum analyzer in the fixed frequency mode, and to measure the signal at a fixed very small frequency (about 10 MHz). In this way photoluminescence extremely close to the laser light is studied. We then vary other parameters, either the detuning of the laser from the polariton resonance or the phase of the local oscillator. This allows to explore all the quadrature components present in the emitted noise.

The sample used in these experiments is a high finesse GaAs microcavity containing one InGaAs quantum well with low indium content and described in more detail in Ref. [18]. The Rabi splitting is 2.8 meV. The linewidth (FWHM) of the lower polariton at 4 K is of the order of 200 μeV. The light source is a single-mode tunable cw Ti: sapphire laser with a linewidth of the order of 1 MHz. The spot diameter is 50 μm. In all experiments the lower polariton branch is excited close to resonance at normal incidence with a σ^+ polarized beam.

In order to investigate the emission lineshape close to the polariton resonance, the detuning of the laser from the polariton resonance is scanned, the frequency of the spectrum analyzer and the phase of the local oscillator being kept fixed. The emission lineshape can be studied in the vicinity of the polariton resonance branches either by scanning the laser energy ('vertical' scan in Fig. 7(a)) for fixed positions on the sample or by scanning the position of the laser on the sample ('horizontal' scan in Fig. 7(a)) at fixed laser frequencies. As for the bistability curves, the second procedure was chosen. The position scan amounts to varying the detuning between the polariton and the laser at a fixed laser frequency. An example of such a signal is shown in Fig. 7(b) for very low laser intensity.

At very low driving intensity, the emission exhibits maxima for the same laser frequencies and positions on the sample as the reflectivity minima [33]. We have studied the height of the emission resonance as a function of the driving laser intensity. At low laser excitation, the maximum emission intensity has a linear dependence on the intensity of the driving laser, as is expected from thermal luminescence. When the laser intensity is increased, the emission exhibits a marked threshold. Above threshold, the emitted intensity increases very fast with the driving intensity. The threshold takes place at very low excitation intensities. It is as low as 2 mW of incident laser power over a spot of 80 μm in diameter (20 W/cm^2). The threshold is lowest for values of the cavity–exciton detuning close to zero. All the considered laser intensities correspond to exciton densities that are below the polariton bleaching density.

In a second series of experiments, performed at a fixed detuning, we have studied the phase dependence of the signal. For each value of the local oscillator phase, the emission having a specific phase is singled out by the homodyne detection system. Scanning the local oscillator phase allows us to know, whether some quadrature components are amplified in a preferential way.

Well below threshold, as expected, all quadrature components are equivalent. Starting a little below threshold, one observes an oscillation of the homodyne signal as a function of the local oscillator phase. A typical recording is shown in Fig. 8, at zero cavity–exciton detuning. This clearly demonstrates the phase dependence of the polariton field typical of degenerate parametric amplification [18]. The polariton–polariton interaction, which is at the origin of the observed amplification is a coherent one, which can be identified with polariton four-wave mixing [13].

4.3. Quantum effects in semiconductor microcavities

The recording of Fig. 8 does not show any squeezing. Actually, while the emission is deamplified for some quadrature components, it does not go below the standard quantum noise. Let us first go back to the theoretical prediction that can be made for squeezing in the emitted light. The properties of the light going out of the microcavity are calculated using Eq. (22). The result is shown in Fig. 9. It can be shown that squeezing is predicted only if the

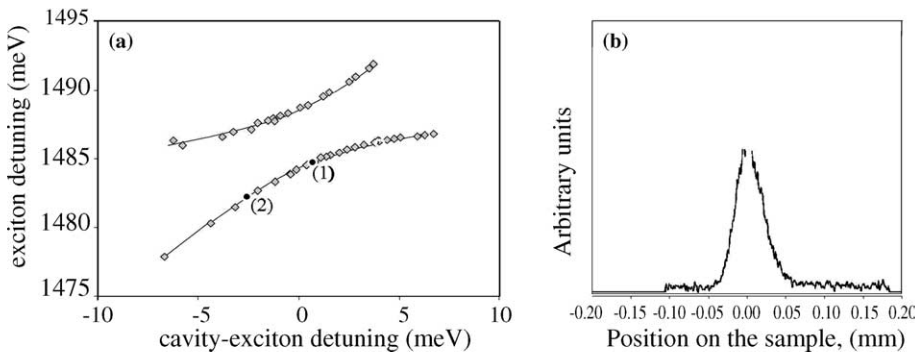

Fig. 7. (a) Experimentally determined energy diagram of the two polariton branches; (b) measured noise when the laser spot position (i.e. the exciton-cavity detuning) is scanned at constant laser frequency. The measurement is made at very low intensity, where there is no non-linear effect.

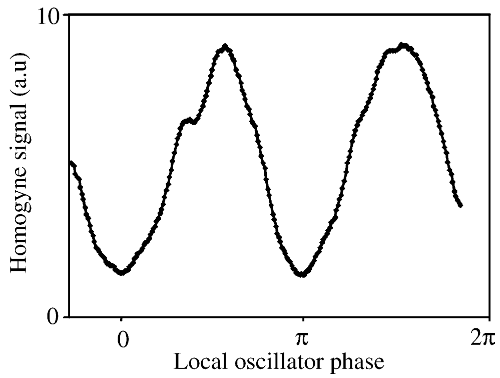

Fig. 8. Noise signal recorded with the homodyne detection system when the phase of the local oscillator is scanned.

parameter β assumes a value smaller than a critical value β_c with $\beta_c = \alpha/2\gamma_{exc}$. The experimentally determined value of $\beta = 0.5\ \beta_c$ is low enough to allow for squeezing.

This treatment ignores other noise sources like the exciton–exciton interaction itself which is at the origin of the coherent non-linear effect but also causes incoherent effects such as broadening and fluctuations. This effect can in principle be calculated from the Hamiltonian [32]. It is, however, quite difficult to evaluate by this method. We have estimated it phenomenologically by using the fluctuation–dissipation theorem. For this, we replace γ_{exc} in Eq. (14) by its value in the presence of collisional broadening, i.e. we take into account the incoherent effect of exciton–exciton interaction, the coherent part of which is accounted for by the second term on the right hand side of Eq. (14). As a result, additional dissipation is included by means of the first term and additional fluctuations are included by means of the last term. Using the measured value of the broadening and $\beta = 0.5\ \beta_c$, we obtain an overall reduced squeezing, compared to the squeezing predicted without broadening. The optimal squeezing value predicted by the phenomenological model under these conditions is about 12%, occuring right below the bistability threshold.

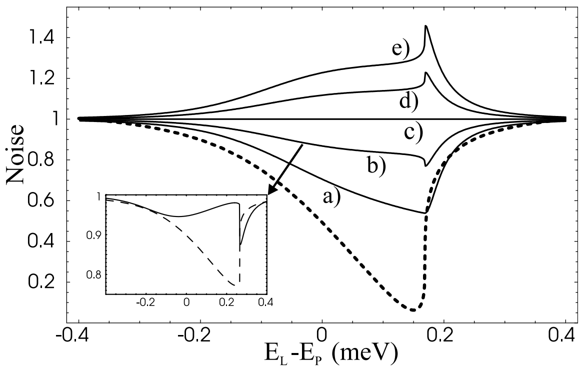

Fig. 9. Solid line: minimal noise S of the reflected light (normalized to standard quantum noise) at zero noise frequency versus the laser-polariton energy detuning $E_L - E_P$, for various values of the excess-noise parameter: (a) $\beta = 0$, (b) $\beta = 0.5\ \beta_c$, (c) $\beta = \beta_c$, (d) $\beta = 1.5\ \beta_c$, (e) $\beta = 2\ \beta_c$. Dashed line: reflectivity. Other parameters: cavity–exciton detuning $\delta = 0$, input intensity I_1^{in} is equal to the bistability threshold intensity. Curve (c) is indistinguishable from the horizontal axis $S_{min} = 1$. Inset: minimal noise obtained with $\beta = 0.5\ \beta_c$, and including the effect of collisional broadening. The exciton linewidth is $\gamma_{exc}(\mu eV) = 75 + 1.8 \times 10^3 n_b$, where n_b is the exciton mean number, accounting for the measured dependence of the polariton linewidth on the density of excitation.

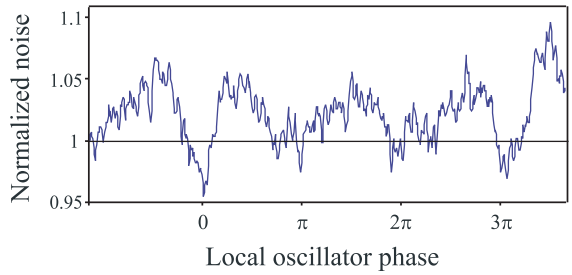

Fig. 10. Noise signal measured with the homodyne detection, normalized to standard quantum noise, when the local oscillator phase is varied allowing to explore all the quadrature components of the noise. The origin of the horizontal axis is arbitrary. Rather large variations are seen from one period to the next because of mechanical vibrations. The cavity–exciton detuning is 0.3 meV and the excitation intensity is 2.2 mW.

According to the above model, the best squeezing rate is expected in the vicinity of a turning point of bistability, as in other non-linear systems (see for example [27]). Therefore noise measurements were performed close to the turning points, where the resonance region is dot-shaped. In order to better isolate the light emitted by the sample area, where the non-linear interaction takes place, spatial filtering was implemented in the way described above. By this method, one avoids averaging of the signal over the whole reflected beam.

The resulting noise signal is shown in Fig. 10. After corrections for detection efficiency, a squeezing in the reflected field of $4 \pm 2\%$ is measured. Squeezing is achievable only in a narrow range of detunings and laser intensities below the bistability threshold. The order of magnitude is in fair agreement with the experimental value, in view of the approximations made in the model.

From the measurement of the reflected field fluctuations we deduce a squeezing of 6% of the internal polariton field using the method of Ref. [36]. In contrast to the case of a Kerr medium in a cavity, the squeezing of the reflected field is smaller than the internal mode squeezing, because the squeezed mode is a polariton mode and not a photon mode, which causes additional losses at the output of the cavity (since only the photon fraction of the polariton goes through the cavity mirror). In some way, measuring the output light field is like looking at the polariton mode through a beamsplitter with an amplitude transmission coefficient equal to C_0 (the Hopfield coefficient representing the photon fraction of the polariton) which leads to a reduction of the measured squeezing with respect to the internal polariton squeezing.

In conclusion, we have presented a study of the non-linear emission of the semiconductor microcavity and shown the phase dependence of the emission due to parametric processes. We have reported the generation of squeezed polaritons in semiconductor microcavities, using polariton degenerate four-wave mixing. The polariton squeezing generates squeezing of the outgoing light, which is measured to be 4%. The squeezing was obtained just above the bistability threshold, close to a turning point, and the bistable region was selected by spatial filtering. A squeezing of 6% of the part-light, part-matter polariton field can be inferred from the measurements. This result opens the way to the generation of non-classical states of light and matter in semiconductor microcavities. Such non-classical effects should also be observed in non-degenerate four-wave mixing, since quantum correlations between the polariton signal and idler fields have been recently predicted [37].

References

[1] C. Weisbuch, M. Nishioka, A. Ishikawa, Y. Arakawa, Phys. Rev. Lett. 69 (1992) 3314; R. Houdré, C. Weisbuch, R.P. Stanley, U. Oesterle, P. Pellandini, M. Ilegems, Phys. Rev. Lett. 73 (1994) 2043.
[2] H. Benisty, et al., Confined Photon Systems, Springer, Berlin, 1999.
[3] H. Cao, et al., Phys. Rev. A 55 (1997) 4632.
[4] L.S. Dang, et al., Phys. Rev. Lett. 81 (1998) 3920; F. Boeuf, et al., Phys. Rev. B 62 (2000) R2279.
[5] P. Senellart, J. Bloch, Phys. Rev. Lett. 82 (1999) 1233.
[6] P.G. Savvidis, J.J. Baumberg, R.M. Stevenson, M.S. Skolnick, D.M. Whittaker, J.S. Roberts, Phys. Rev. Lett. 84 (2000) 1547.
[7] R. Huang, F. Tassone, Y. Yamamoto, Phys. Rev. B 61 (2000) R7854.
[8] R. Houdré, C. Weisbuch, R.P. Stanley, U. Oesterle, M. Ilegems, Phys. Rev. Lett. 85 (2000) 2793.
[9] R.M. Stevenson, V.N. Astratov, M.S. Skolnick, D.M. Whittaker, M. Emam-Ismail, A.I. Tartakovskii, P.G. Savvidis, J.J. Baumberg, J.S. Roberts, Phys. Rev. Lett. 85 (2000) 3680.
[10] C. Ciuti, P. Schwendimann, B. Deveaud, A. Quattropani, Phys. Rev. B 62 (2000) R4825.
[11] M. Kuwata-Gonokami, et al., Phys. Rev. Lett. 79 (1997) 1341.
[12] F. Quochi, et al., Phys. Rev. B 159 (1999) R15594.
[13] A. Yariv, Quantum Electronics, 3rd ed., Wiley, New York, 1989 (Chapter 17).
[14] Y. Mu, C.M. Savage, J. Opt. Soc. Am. B, 965; M.O. Scully, M.S. Zubairy, Quantum Optics, Cambridge University Press, New York, 1995 (Chapter 21).
[15] G. Messin, J.P. Karr, H. Eleuch, J.M. Courty, E. Giacobino, J. Phys. Condens. Matter 11 (1999) 6069; H. Eleuch, J.M. Courty, G. Messin, C. Fabre, E. Giacobino, J. Opt. B: Quantum Semiclass. Opt. 1 (1999) 1.
[16] R.E. Slusher, et al., Phys. Rev. Lett. 55 (1985) 2409.
[17] A.M. Fox, J.J. Baumberg, M. Dabbicco, B. Huttner, J.F. Ryan, Phys. Rev. Lett. 74 (1995) 1728.
[18] G. Messin, J.Ph. Karr, A. Baas, G. Khitrova, H. Gibbs, R. Houdre, R.P. Stanley, U. Oesterle, E. Giacobino, Phys. Rev. Lett. 87 (2001) 127403.
[19] J.Ph. Karr, A. Baas, R. Houdre, E. Giacobino, Phys. Rev. A 69 (2004) R031802.
[20] G. Bastard, Wave Mechanics Applied to Semiconductor Heterostructures, Editions de Physique, Les Ulis, Paris, 1989.
[21] V. Savona, L.C. Andeani, P. Schwendimann, A. Quattropani, Solid State Commun. 93 (1995) 733.
[22] S. Haroche, Cavity quantum electrodynamics in: J. Dalibard, J.M. Raymond, J. Zinn-Justin (Eds.), Fundamental Systems in Quantum Optics, London Science Publishers, Amsterdam, 1992.
[23] Cavity quantum optics and the quantum measurement process, Progress in Optics XXX, 261 (1992).
[24] E. Hanamura, J. Phys. Soc. Jpn. 1545 (1974) (1974) 37; E. Hanamura, J. Phys. Soc. Jpn. 1553 (1974) 1553.
[25] H. Haug, Z. Phys. B 24 (1976) 351.
[26] M.J. Collett, C.W. Gardiner, Phys. Rev. A 30 (1984) 1386; S. Reynaud, A. Heidmann, Opt. Commun. 71 (1989) 209.
[27] L. Hilico, et al., Phys. Rev. A 46 (1992) 4397.
[28] A. Tredicucci, et al., Phys. Rev. A 54 (1996) 3493.
[29] X. Chen, et al., J. Opt. B: Quantum Semiclass. Opt. 1 (1999) 524.
[30] B.G. Sfez, J.L. Oudar, J.C. Michel, R. Kuszelewicz, R. Azoulay, Appl. Phys. Lett. 57 (1990) 324.
[31] A. Baas, J.Ph. Karr, H. Eleuch, E. Gardiner, Phys. Rev. A 69 (2004) 023809.
[32] M.L. Steyn-Ross, C.W. Gardiner, Phys. Rev A 27 (1983) 310.
[33] R.P. Stanley, et al., Phys. Rev. B 55 (1997) R4867.
[34] H.P. Yuen, V.W.S. Chan, Opt. Lett. 8 (1983) 177.
[35] H.A. Bachor, A Guide to Experiments in Quantum Optics, Wiley, Weinheim, 1998 (p. 181–183).
[36] C.W. Gardiner, P. Zoller, Quantum Noise, Springer, Berlin, 2000 (p. 326–328).
[37] P. Schwendimann, C. Ciuti, A. Quattropani, Phys. Rev. B 68 (2003) 165324; J.Ph. Karr, A. Baas, R. Houdré, E. Grocobino, Phys. Rev. B69 (2004) 063807.